Optical injection probing of single ZnO tetrapod lasers

Jodi M. Szarko [a,1], Jae Kyu Song [a], Charles Wesley Blackledge [a], Ingmar Swart [a], Stephen R. Leone [a,*], Shihong Li [b], Yiping Zhao [b]

[a] *Departments of Chemistry and Physics, and Lawrence Berkeley National Laboratory, University of California, Berkeley, California 94720*

[b] *Department of Physics and Astronomy, University of Georgia, Athens, Georgia 30602*

Abstract

The properties of zinc oxide (ZnO) nanotetrapod lasers are characterized by a novel ultrafast two-color pump/stimulated emission probe technique. Single legs of tetrapod species are isolated by a microscope objective, pumped by 267 nm pulses, and subjected to a time-delayed 400 nm optical injection pulse, which permits investigation of the ultrafast carrier dynamics in the nanosize materials. With the optical injection pulse included, a large increase in the stimulated emission at 400 nm occurs, which partially depletes the carriers at this wavelength and competes with the normal 390 nm lasing. At the 390 nm lasing wavelengths, the optical injection causes a decrease in the stimulated emission due to the energetic redistribution of the excited carrier depletion, which occurs considerably within the time scale of the subpicosecond duration of the injection pulse. The effects of the optical injection on the spectral gain are employed to probe the lasing dynamics, which shows that the full width at half maximum of the lasing time is 3 ps.

* Corresponding author. Fax: +1-510-643-1376.

E-mail address: srl@berkeley.edu (S.R. Leone)

[1] also with Department of Chemistry and Biochemistry, University of Colorado, Boulder, Colorado, 80309

1. Introduction

For the past few years, the lasing characteristics in ZnO films [1,2] and powders [3] have been widely investigated. These studies, along with the discovery and understanding of single nanowire lasers [4], have led to a number of investigations pertaining to the growth and characterization of ZnO microcavity lasers [5,6]. However, only a few studies have been reported on the dynamic response of ZnO microcavity lasers [7], although such studies would afford excellent means to probe the carrier dynamics in the nanostructure lasers. In addition, the understanding of the response of the carrier distribution to the strong optical fields in semiconductor lasers is essential for optimizing the performance of these devices. While many important ultrafast laser experimental techniques are used to interrogate time-resolved semiconductor material dynamics, these methods have not been applied to single nanostructured devices as readily because of the low signal-to-noise ratios. The stimulated emission pump-probe method is a robust way to begin interrogating these nanostructures, which permits investigation of the lasing in fragile and difficult-to-access nanoscale crystalline materials and nanoresonators. In this letter, we report the effect of time-delayed external optical injection pulses on single-species ZnO tetrapod structures during lasing. Both temporal and spectral maps of the effect of the optical injection pulse on the normal stimulated emission are obtained. This method shows promise for determining the energetic redistribution of carriers and its effect on quenching and gain in free-standing microcavity lasers as well as on the lasing dynamics.

2. Experiments

ZnO tetrapods are grown with a vapor phase transport process by heating Zn powder to 700º C in a quartz tube furnace with an argon flow of 300 sccm under ambient pressure. The

shapes and lengths of the tetrapods are characterized by scanning electron microscopy and optical microscopy. The diameters of the legs of the tetrapods are distributed between 200 and 800 nm, and the lengths of the legs are typically in the range of 10-30 μm. X-ray diffraction and scanning electron microscopy measurements demonstrate the hexagonal wurtzite structures of the legs in tetrapods [8,9]. The tetrapods are sonicated in methanol to isolate individual tetrapods, and the methanol solution is drop-coated onto quartz or glass substrates.

The experimental setup for the ultrafast pump-probe experiments is presented in Fig. 1. Single tetrapods are excited with the third harmonic (267 nm) of a regeneratively amplified Ti:sapphire laser (nominally 150 fs, 250 kHz, 2 μJ/pulse) and probed with a second harmonic (400 nm) pulse. The cross-correlation between the pump and probe pulse is 300 fs. Both beams are focused onto a single tetrapod or a single leg of a tetrapod using a UV microscope objective. The ZnO spontaneous and laser emission, along with the scattered and reflected light of the probe, are collected by the same objective and spectrally resolved using a monochromator. This light is detected using a photomultiplier tube (PMT) with lock-in detection or a charge-coupled device. Time-resolved pump-probe experiments are carried out by varying the time delay of the 400 nm probe pulse with respect to the 267 nm pump pulse with a computer-controlled variable delay stage, where the intensity of the probe is collected through the monochromator while chopping the pump.

In the optical gain spectrum, the time-delayed 400 nm pulse is employed as an optical injection pulse rather than a probe, which can be regarded as a stimulating pulse. The spectrally-resolved optical gain spectrum is obtained at the selected delay time of the optical injection, while chopping the 400 nm optical injection and collecting the integrated signal with the PMT/lock-in amplifier as the monochromator is scanned. A spectrum is also obtained with the

optical injection only and subtracted from the pump/injection spectrum to remove the large scattered signal of the optical injection pulse. The time-resolved optical gain spectrum is acquired by measuring the emission at the wavelengths corresponding to normal laser modes, while chopping and varying the time delay of the 400 nm optical injection. Using these experimental methods, the spectral and temporal changes in the sample under stimulated emission conditions are obtained.

3. Results and discussion

The emission spectra as a function of excitation intensity for a single leg of a nanotetrapod isolated by the microscope objective are shown in Fig. 2(a). At low excitation intensity (10 $\mu J/cm^2$), a broad photoluminescence is observed. When the excitation intensity is above the lasing threshold (12 $\mu J/cm^2$), sharp peaks grow in, which are from the longitudinal lasing modes of an individual resonator structure. The spectral spacing of the longitudinal modes is 1.5 nm, which corresponds to a 20 μm resonator length, according to the equation $\Delta\lambda = \lambda^2/2nL$ [10], where n is the refractive index of ZnO and L is the cavity length. This length, compared to the length of the tetrapod species, suggests that the resonator is formed in only one leg of the tetrapod structure. The superlinear increase of the emission intensity is observed at excitation intensities > 12 $\mu J/cm^2$, where the sharp peaks grow in, as shown in the inset of Fig. 2(a). The lasing threshold is dependent upon the properties of the tetrapods such as the dimensions, end facet quality, and substrate coupling. A lasing threshold as low as 5 $\mu J/cm^2$ was found for one tetrapod. At low excitation intensities, lasing occurs at the same wavelengths over a range of excitation intensities, implying the exciton-exciton scattering mechanism for lasing. On the other

hand, as the excitation intensity is further increased into the electron-hole plasma (EHP) regime, the lasing becomes red-shifted due to the band gap renormalization [6,11], as shown in Fig 2(b).

In order to investigate the ultrafast carrier dynamics during the lasing, time-resolved pump-probe experiments are carried out, one of which is presented in Fig. 3. The intensity of the pump pulse is 80 $\mu J/cm^2$, and the carrier density is initially in the EHP regime. At the probe wavelength of 400 nm, the temporal signal maps out the carrier dynamics corresponding to this wavelength. The subpicosecond decrease of the probe observed near zero time is assigned to hot carrier absorption. After a rise time of 1 ps, the stimulated emission by the probe pulse is maximized. The rise time seems to have a close relationship with the formation of the EHP. The buildup of the EHP is a cooling process from hot carriers to a quasi-thermalized system with a cooling time of 1 ps, which renormalizes the band gap and is accompanied by a red-shift [12]. After the quasi-equilibrium, the carriers follow a biexponential decay with time constants of 5 and 50 ps, which represent the decays of the EHP and the excitonic carriers, respectively [7,13].

The optical gain spectrum (solid line) of a single leg of a tetrapod obtained at a time of 2 ps for the delayed optical injection (400 nm) after the excitation (267 nm) is presented in Fig. 4; at this time delay the stimulated emission by the optical injection pulse is maximized. The intensity of the pump pulse is also 80 $\mu J/cm^2$. The carrier density is estimated to be $\sim 5 \times 10^{18}$ cm^{-3}, which is in the EHP regime [14]. The wavelength of the optical injection pulse overlaps with the long wavelength tail of the emission spectrum, and the effect of the optical injection on the total spectrum is examined. Three sharp dips are observed along with a much smaller decrease in other wavelengths, as shown in Fig. 4(a). Along with the dips, a strong increase of emission appears at the 400 nm injection wavelength. Initially, the injection pulse induces

stimulated emission and creates more 400 nm photons, which therefore depletes the carriers near the band gap edge.

To better characterize the effect of the injection pulse on the nanostructure laser medium, the change in the carrier density due to the injection is estimated by the rate of carrier depletion. If we can assume that complete electronic redistribution occurs, the rate equation has the form [15]:

$$\frac{dN}{dt} = -\left[S(N) + \gamma_s N + \gamma_{nr} N + \frac{G(\lambda,t)I}{h\nu} \right] \qquad (1)$$

where N is the carrier density, $S(N)$ is the lasing emission rate, γ_s is the spontaneous emission rate constant, γ_{nr} is a nonradiative rate constant, $G(\lambda,t)$ is the gain at the optical injection wavelength, I is the optical injection intensity, and $h\nu$ is the photon energy of the optical injection. Since the pulse width of the optical injection is much shorter than the decay time of the carriers, only the last term of (1) is taken into account for simplicity. When a gain value for thin films of ZnO in the EHP regime is used, 2000 cm^{-1} at the temporal gain maximum [13], the change in the carrier density due to the 400 nm optical injection pulse is approximated to be 4×10^{17} cm^{-3} for this structure. The narrow depletion of carriers is energetically redistributed by carrier-carrier and carrier-phonon scattering processes [15-17]. Therefore, the superlinear lasing emission at 390 nm, attributed to the carrier density and its change, gives rise to a distinctive decrease of the lasing even with only a small depopulation of the carrier density. This permits an estimate of the effective carrier density change by the optical injection in our experiments. The dependence of the lasing intensity on the excitation intensity (and therefore the carrier density), similar to the dependence shown in the inset of Fig. 2(a), is obtained. The change in the lasing intensity by the optical injection at 2 ps is measured at the three lasing modes and compared to the lasing

intensities without the injection. The effective loss in carrier density is estimated to be 2×10^{17} cm^{-3} for this structure under these pump conditions, which is the same order of magnitude as the change obtained by the model. The modest difference may originate from the assumption of complete and rapid electronic redistribution in the model or a difference in the value used for the gain. However, the results suggest that there is a considerable amount of energetic redistribution within the duration of the injection pulse, which leads to a rapid nearly quasi-thermalized distribution of the carrier densities, but possibly not a totally homogeneous redistribution of states.

For comparison, the time-integrated emission spectrum (dotted line in Fig. 4) is obtained with the pump only, and this is presented with the magnified negative value of the gain in the inset of Fig. 4(a). Both the emission and gain spectra have peaks at the same wavelengths, proving that the dips originate from the longitudinal modes of lasing. It is worth noting that the peaks in the gain spectrum are narrower than those in the emission spectrum. The lasing is more distinctive in the gain spectrum due to the superlinearity of the lasing, whereas photoluminescence and amplified spontaneous emission contribute to the emission spectrum even in these lasing tetrapod legs due to the intrinsic low reflectivity of the end facets of ZnO nanowires (20 %) [6]. When the lasing is predominant and the photoluminescence and amplified spontaneous emission are scant, as shown in Fig. 4(b), the gain spectrum exhibits almost an identical spectral shape to the emission spectrum. Therefore, this optical gain spectrum can be used as a novel method to distinguish the lasing from other emissions.

The ultrafast lasing dynamics of single lasing ZnO tetrapods can be investigated using the transient effect of the optical injection on the spectral gain, which is presented in Fig. 5(a). The temporal profile at 391 nm represents the lasing dynamics of this lasing mode, which is probed

as the delay of the injection (400 nm) is varied. The decrease of the lasing is faster than the carrier density decay of the EHP, as shown in the inset of Fig 5(a). In order to understand the temporal profile of lasing at 391 nm, the rate equation for a semiconductor laser is employed, which has the form [18]:

$$\frac{dP}{dt} = [g(N) - \gamma]P + R_{sp}(N) \qquad (2)$$

where P is the photon density, $g(N)$ is the gain, N is the carrier density, γ includes the internal loss and end facet loss, and R_{sp} is the rate of spontaneous emission. Because the intensity of the spontaneous emission at the lasing wavelengths is much smaller than that of the lasing, only the first term, $[g(N) - \gamma]P$, of (2) is taken into account for the simple estimation. With the assumption that γ is independent of the carrier and photon density, the best fit is obtained with rise and fall times of 1.0 ps and 1.1 ps, respectively, as shown in Fig. 5(b). The fall time of the lasing is much faster than the EHP decay, primarily due to the superlinearity of the emission gain in the lasing, which is strongly dependent upon the carrier density. The full width at half maximum of the lasing duration time is 3 ps, which is, to our knowledge, the shortest lasing generated from such microcavity lasers [19].

4. Conclusions

Lasing is studied in the individual legs of ZnO tetrapods by the novel method of pump/optical injection as well as pump/stimulated emission probe spectroscopy. The spectral changes in the emission due to an injection pulse show a large increase at the injection wavelength and a distinctive decrease in the longitudinal modes of lasing. This decrease by the optical injection pulse is used to estimate the electronic redistribution rate of the structures and the lasing dynamics. It can be concluded that a considerable amount of energetic redistribution of

the excited carrier population occurs within the duration of the injection pulse. The fall time of the lasing is much faster than the carrier decay time due to the superlinearity of the lasing, which is related to the carrier density.

Acknowledgments

The initial lasing experiments were supported by an exploratory grant from the National Science Foundation, ECS-0210106. Construction of the laboratories, additional equipment, and support were provided by the Director, Office of Science, Office of Basic Energy Sciences, Materials Science Division, U.S. Department of Energy under contract No. DE-AC03-76SF00098. The National Institute of Standards and Technology provided some instruments for this work on loan. JKS was partially supported by the Post-Doctoral Fellowship Program of the Korea Science and Engineering Foundation. SHL and YPZ were supported by the National Science Foundation under contract No. ECS-0304340.

References

[1] D.M. Bagnall, Y.F. Chen, Z. Zhu, T. Yao, S. Koyama, M. Y. Shen, T. Goto, Appl. Phys. Lett. 73 (1998) 1038.

[2] D.C. Reynolds, D.C. Look, B. Jogai, Solid State Comm. 99 (1996) 873.

[3] H. Cao, J.Y. Xu, E.W. Seelig, R.P.H. Chang, Appl. Phys. Lett. 76 (2000) 2997.

[4] J. Hu, T.W. Odom, C.M. Lieber, Acc. Chem. Res. 32 (1999) 435.

[5] M.H. Huang, S. Mao, H. Feick, H. Yan, Y. Wu, H. Kind, E. Weber, R. Russo, P. Yang, Science 292 (2001) 1897.

[6] J.C. Johnson, H. Yan, P. Yang, R.J. Saykally, J. Phys. Chem. B 107 (2003) 8816.

[7] J.C. Johnson, K.P. Knutsen, H. Yan, M. Law, P. Yang, R.J. Saykally, Nano Letters 4 (2004) 197.

[8] Z. Chen, Z. Shan, M.S. Cao, L. Lu, S.X. Mao, Nanotechnology 15 (2004) 365.

[9] Y.H. Leung, A.B. Djurišić, J. Gao, M.H. Xie, W.K. Chan, Chem. Phys. Lett. 385 (2004) 155.

[10] B.E.A. Saleh, M.C. Teich, *Fundamentals of Photonics* (John Wiley & Sons, Inc., New York, 1991).

[11] Z.K. Tang, G.K.L. Wong, P. Yu, M. Kawasaki, A. Ohtomo, H. Koinuma, Y. Segawa, Appl. Phys. Lett. 72 (1998) 3270.

[12] J. Takeda, H. Jinnouchi, S. Kurita, Y.F. Chen, T. Yao, Phys. Stat. Sol. (b) 229 (2002) 877.

[13] A. Yamamoto, T. Kido, T. Goto, Y. Chen, T. Yao, A. Kasuya, Appl. Phys. Lett. 75 (1999) 469.

[14] K. Postava, H. Sueki, M. Aoyama, T. Yamaguchi, C. Ino, Y. Igasaki, M. Horie, J. Appl. Phys. 87 (2000) 7820.

[15] A.P. de Boer, P.C.M. Christianen, J.C. Maan, T. Rasing, V.I. Tolstikhin, T.G. van de Roer, H.M. Vrieze, Appl. Phys. Lett. 72 (1998) 2936.

[16] J. Shah, *Ultrafast Spectroscopy of Semiconductors and Semiconductor Nanostructures*, Vol. 115 (Springer, Heidelberg, 1996).

[17] A. Othonos, J. Appl. Phys. 83 (1998) 1789.

[18] G.P. Agrawal, G.R. Gray, Appl. Phys. Lett. 59 (1991) 399.

[19] P. Michler, M. Hilpert, W.W. Rühle, H.D. Wolf, D. Bernklau, H. Riechert, Appl. Phys. Lett. 68 (1996) 156.

Figure captions

Fig. 1. Schematic diagram of the experimental setup for pump-probe and pump-optical injection experiments. The fundamental 800 nm beam was generated by a regeneratively amplified Ti-sapphire laser, which is doubled and tripled to obtain the probe and pump beam, respectively. The inset shows an optical microscope image of a ZnO tetrapod.

Fig. 2. Excitation intensity dependence of the emission and lasing in a ZnO tetrapod with 267 nm excitation. (a) The broad photoluminescence is observed at low excitation intensity. As the excitation intensity increases above the lasing threshold, sharp lasing peaks grow in at several wavelengths. The inset shows the superlinear increase of the emission intensity above the lasing threshold. (b) The lasing becomes red-shifted due to the band gap renormalization, as the excitation intensity is further increased into the electron-hole plasma regime, after the initial exciton-exciton stimulated emission regime.

Fig. 3. Time-resolved temporal profile at 400 nm obtained by a pump (267 nm)-probe (400 nm) experiment at the pump intensity of 80 $\mu J/cm^2$.

Fig. 4. The optical gain spectra (solid lines) for a single lasing tetrapod structure obtained with the pump and optical injection pulse and the emission spectra (dotted lines) obtained only with the pump pulse. (a) The optical gain spectrum shows three sharp dips at the lasing modes and the stimulated emission at 400 nm. The inset shows the magnified negative value of the gain spectrum. (b) The optical gain spectrum of a different tetrapod shows two sharp dips at the lasing modes. The inset shows the magnified negative value of the gain spectrum.

Fig. 5. (a) Transient profiles at several wavelengths with the 400 nm injection. At 391 nm, the temporal profile is primarily characterized by the timescale of the lasing of the mode at that wavelength. The inset shows the normalized negative value of the transient profile at 391 nm. (b) Time evolution of the measured (solid line) and fitted (dotted line) lasing from a single tetrapod laser. The full width at half maximum of the lasing time is 3 ps.

FIG. 1.

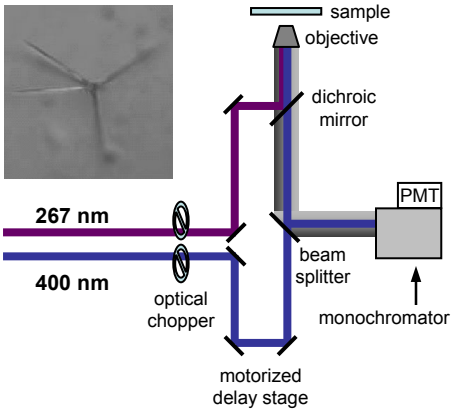
sample
objective
dichroic
mirror
PMT
267 nm
400 nm
optical
chopper
beam
splitter
monochromator
motorized
delay stage

FIG. 2.

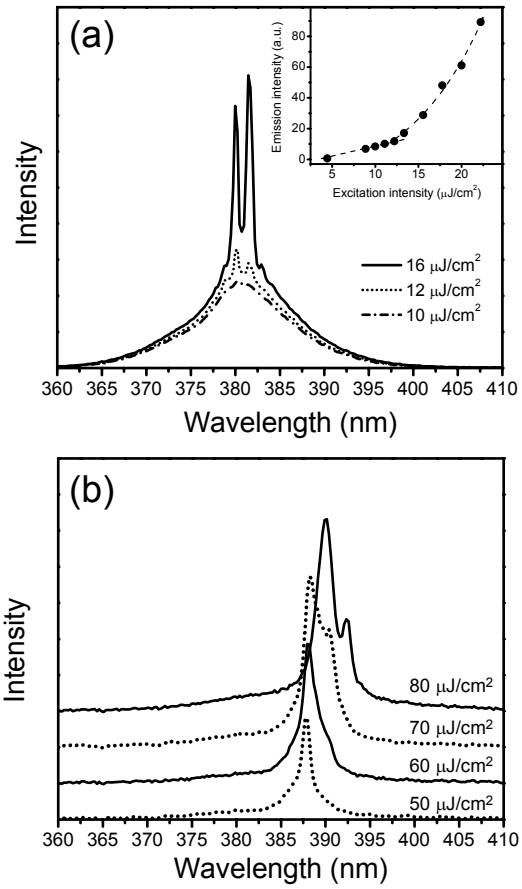
(a)
Intensity
Wavelength (nm)
360 365 370 375 380 385 390 395 400 405 410
Emission intensity (a.u.)
0 20 40 60 80
5 10 15 20
Excitation intensity (μJ/cm²)
16 μJ/cm²
12 μJ/cm²
10 μJ/cm²
(b)
Intensity
Wavelength (nm)
360 365 370 375 380 385 390 395 400 405 410
80 μJ/cm²
70 μJ/cm²
60 μJ/cm²
50 μJ/cm²

FIG. 3.

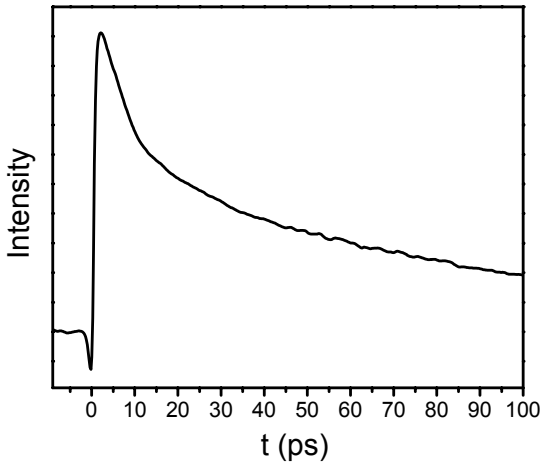

FIG. 4.

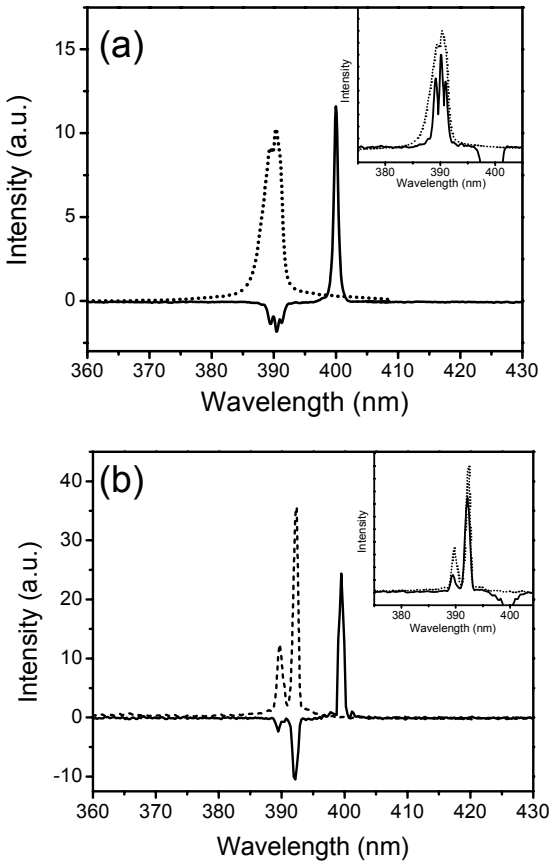
(a)
Intensity (a.u.)
15
10
5
0
360
370
380
390
400
410
420
430
Wavelength (nm)
Intensity
380
390
400
Wavelength (nm)
(b)
Intensity (a.u.)
40
30
20
10
0
-10
360
370
380
390
400
410
420
430
Wavelength (nm)
Intensity
380
390
400
Wavelength (nm)

FIG. 5.

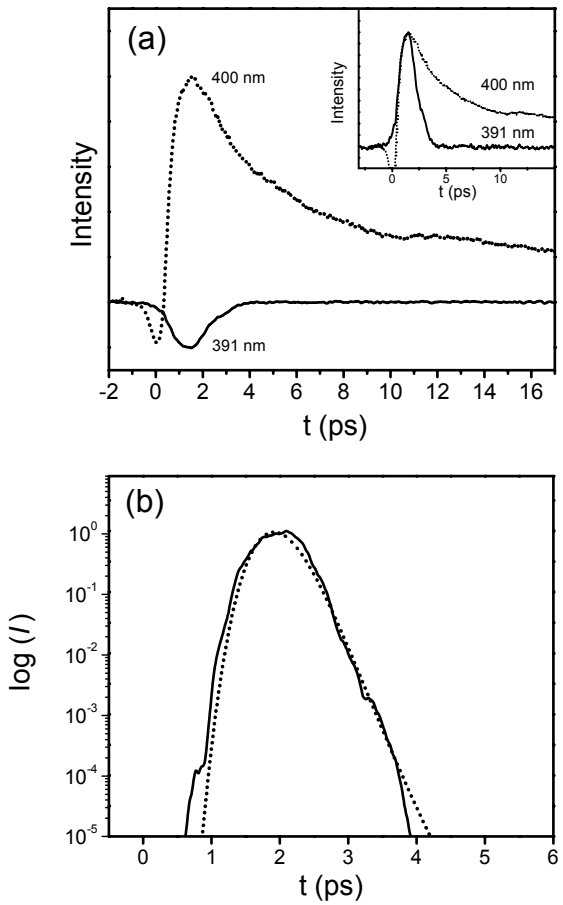
(a)
400 nm
391 nm
Intensity
-2 0 2 4 6 8 10 12 14 16
t (ps)
Intensity
400 nm
391 nm
0 5 10
t (ps)
(b)
log (I)
10^{0}
10^{-1}
10^{-2}
10^{-3}
10^{-4}
10^{-5}
0 1 2 3 4 5 6
t (ps)